www.czasopisma.pan.pl PAN POLSKA AKADEMIA NAUK www.journals.pan.pl

A R C H I V E S O F M E T A L L U R G Y A N D M A T E R I A L S

Volume 60 2015 Issue 4

DOI: 10.1515/amm-2015-0478

M. KRÓL*,#, T. TAŃSKI*, G. MATULA*, P. SNOPIŃSKI*, A.E. TOMICZEK*

ANALYSIS OF CRYSTALLISATION PROCESS OF CAST MAGNESIUM ALLOYS BASED ON THERMAL DERIVATIVE ANALYSIS

ANALIZA PROCESU KRYSTALIZACJI ODLEWNICZYCH STOPÓW MAGNEZU W OPARCIU O ANALIZĘ TERMICZNO-DERYWACYJNĄ

The paper presents the results of the crystallisation process of cast magnesium alloys based on the thermal-derivation analysis.

The effects of aluminium content and cooling rate on the characteristic parameters of the evaluation of magnesium dendrites during solidification at different cooling rates were investigated by thermal-derivative analysis (TDA). Dendrite coherency point (DCP) is defined with a new approach based on the second derivative cooling curve. Solidification behaviour was evaluated via one thermocouple thermal analysis method. Microstructural evaluations were characterised by light microscope, X-ray diffraction, scanning electron microscopy, and energy dispersive X-ray spectroscopy. This research revealed that utilisation of d^2T/dt^2 versus the time curve methodology allows for analysis of the dendrite coherency point.

Keywords: cast magnesium alloys, crystallisation, thermal derivative-analysis, the dendrite coherency point

W pracy przedstawiono wyniki badań opisu procesu krystalizacji odlewniczych stopów magnezu w oparciu o analizę termiczno-derywacyjną. Przedstawiono wpływ szybkości chłodzenia oraz stężenia aluminium na charakterystyczne temperatury podczas krystalizacji, jak również wyniki obliczeń udziału frakcji stałej w punkcie koherencji fazy α w oparciu o analizę krzywej d^2T/dt^2, bazując na pomiarze temperatury jedną termoparą. Przedstawiono i omówiono wyniki wpływu szybkości chłodzenia na charakterystyczne temperatury procesu krystalizacji odlewniczych stopów magnezu. Wpływu założonych szybkości chłodzenia na mikrostrukturę dokonano w oparciu o wyniki badań z wykorzystaniem mikroskopii świetlnej oraz mikroanalizy rentgenowskiej jakościowej i ilościowej z wykorzystaniem elektronowej mikroskopii skaningowej. Przedstawiono wyniki badań składu fazowego w oparciu o rentgenowską jakościową analizę fazową.

1. Introduction

Magnesium is one of the lightest materials currently used for structural applications. Because of its exceptional properties like high strength to density ratio, high elasticity, good noise and dampening characteristics its usage has increased in recent years. It is expected that the production of primary magnesium will increase in the future because of CO_2 reduction requirement. Also, magnesium is 6th most abundant metal on the earth, and the recycling possibilities are satisfactory, so that element could become a crucial resource soon. Because pure magnesium is rarely used for applications where high mechanical properties are required, a lot of alloying elements – like aluminium, manganese, zinc or zirconium – were added to magnesium to improve the strength of the material and to extend the range of applications [1-3].

Application of magnesium alloys leads to lowering the fabrication related costs; substitution by lightweight materials leads to secondary weight savings, which allow a lifetime fuel costs reduction. It is also known that the total lifecycle cost of a magnesium part is lower than that of one made from other materials. Hence, the development of new magnesium-based alloys that have better properties and formability could enable greater cost reduction [4-6].

Magnesium alloys are commonly used in the manufacturing of cast engines and transmission housings. Control of the cast structure is one of the most significant requirements in the foundry industry. Castability is affected significantly by the dendrite coherency point (DCP), which expresses the temperature, time and solid fraction at which an interlocking stable network forms during solidification. An increase in the solid fraction at coherency may improve the casting properties of the alloy and reduce casting defects. The DCP is a fundamental characteristic of as-cast alloys, because it indicates the transition from mass to interdendritic feeding during crystallisation [1, 4, 7]. Casting defects, such as macrosegregation, shrinkage, porosity and hot tearing begins below the DCP [4, 8-10]. Consequently, a thorough

* SILESIAN UNIVERSITY OF TECHNOLOGY, INSTITUTE OF ENGINEERING MATERIALS AND BIOMATERIALS, FACULTY OF MECHANICAL ENGINEERING, 18 A KONARSKIEGO STR., 44-100GLIWICE, POLAND

Corresponding author:mariusz.krol@polsl.pl

understanding of solidification behaviour at the DCP and the factors that affect it, are necessary for improving new commercial alloys. Although the DCP is a physical phenomenon, its direct disclosure is virtually impossible. Therefore, indirect methods, such as computer-aided cooling curve analysis (CA-CCA) are used to determine the dendrite coherency point.

The correlation between the cooling curve, crystallisation curve, microstructure, solid fraction, dendrite coherency point is presented and discussed.

2. Experimental procedure

The alloys used in the experiments were MC MgAl6Zn1 and MC MgAl9Zn1 magnesium alloys in the as-cast state. The chemical compositions of the experimental alloys are presented in Table 1. The material has been cast in dies with bentonite binder and shaped into plates of 250x150x25 mm. The experiments were performed using a cylindrical test sample with diameter of 18 mm and length equals to 20 mm, taken from the ingot. Every sample had a predrilled hole to accommodate the supersensitive K-type thermocouple (with the extra low thermal time constants) to collect the thermal data and control the processing temperature, positioned at the centre of the test sample. The thermal-derivative analysis during melting and solidification cycles was carried out using the Universal Metallurgical Simulator and Analyser (UMSA) [11]. At least three thermal-derivative analysis tests were made for each cooling rate to ensure the reproducibility of the results and the average data were reported.

The melting and solidification operations for the magnesium alloys were carried out using argon as protected atmosphere. The data for thermal analysis (TA) was captured using a high-speed National Instruments Data Acquisition System linked to a personal computer equipped with proprietary software for automated data collection, processing, and analysis.

OriginLab and Fityk data analysis software were used to graph and smoothen the corresponding first and second derivative cooling curves. These curves were used to assess solidification behaviour and to determine any characteristic temperatures. The TA signal in the form of heating and cooling curves was captured through the melting and solidification sequences. The temperature vs. time and first derivative vs. temperature were estimated and plotted. Cooling curves received from the central thermocouple were used to define the solid fraction at the point of coherency. It was done by integrating the difference between its first derivative and base line that assumes that no transformations occur.

The test samples were heated to 700±2ºC and isothermally kept at this temperature for a period of 90s in order to stabilise the melt conditions. The cooling rate during all experiments was kept at approx. 0.6, 1.3 and 2.5°C^{s-1}, where the cooling rate 0.6°C^{s-1} corresponds to freely cooling, without any forced air flow. The cooling rate was estimated as the ratio between the temperature difference between the nucleation and solidus temperatures and the complete solidification time.

Fraction solid (FS) was defined by calculating the whole surface region between the first derivative of the cooling curve and the so-called base line (BL). The BL expresses the theoretical first derivative of the cooling curve that does not manifest phase transformation/metallurgical reactions through the crystallisation process. The area between the two derivative curves (calculated between the liquidus and solidus temperatures) is proportionate to the latent heat of crystallisation of the given alloy. Hence, the latent heat directly given to the test sample affected the fraction liquid development. Similar estimates were completed for the fraction solid, except that fraction solid was proportionate to the latent heat released during the crystallisation [8, 12, 13].

Metallographic specimens were taken from a position near to the thermocouple tip. Specimens were cold mounted and ground on 240#, 320#, 400#, 600# and 1200# SiC abrasive and then finished with 6μm, 3μm and 1μm diamond paste. The polished surfaces were etched with used 5% of molybdic acid, with fresh alcohol repeatedly blotted onto the surface to prevent residue deposits. The observations of the studied cast magnesium alloys have been made on the light microscope LEICA MEF4A, as well as on the electron scanning microscope Zeiss Supra 35. The grain size of the magnesium alloys was analyzed by the standard linear intercept method on images acquired by light microscope.

The X-ray qualitative and quantitative microanalysis, and the analysis of a surface distribution of alloying elements, have been made on the Opton DSM-940 scanning electron microscope (SEM) with the Oxford LINK ISIS energy dispersive spectrometer (EDS) at the accelerating voltage of 20kV. Phase composition was determined by the X-ray diffraction technique utilising the X`Pert apparatus including a copper lamp with 40kV voltage. The estimation was performed by angle range of 2Θ: 30º÷120º.

3. Investigation results

The thermal-derivative analysis has investigated the solidification pathways of Mg-Al-Zn alloys. To examine non-equilibrium solidification characteristics, cooling curve analyses and microscopic studies, which consist of cooling curves, their first derivatives and base lines and the scanning

TABLE 1

Chemical composition of investigated magnesium alloys

The mass concentration of primary elements, %							
Alloy	Al	Zn	Mn	Si	Fe	Mg	Rest
MC MgAl6Zn1	5.624	0.46	0.16	0.034	0.07	93.6	0.052
MC MgAl9Zn1	9.399	0.84	0.24	0.035	0.007	89.4	0.079

electron microscopy images in an as-cast state are shown. In the analysed cast magnesium alloys, four thermal events were observed in the crystallisation curves as shown in Fig. 1 and 2. At the inception of crystallisation of any phase, crystallisation curve increases its value and decreases after the completion of solidification. It appears that the peaks correspond to the crystallisation of primary magnesium dendrites, the formation of secondary phases at the interdendritic regions, the eutectic solidification reaction, and the final solidus reaction, respectively.

a) b)

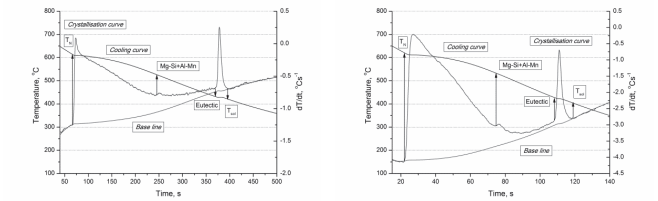

Fig. 1. Representative cooling and its first derivative curves and base line determining the critical points during solidification of the MC MgAl6Zn1 alloy solidify at: a) 0.6°Cs^{-1}; b) 2.5°Cs^{-1} cooling rate

a) b)

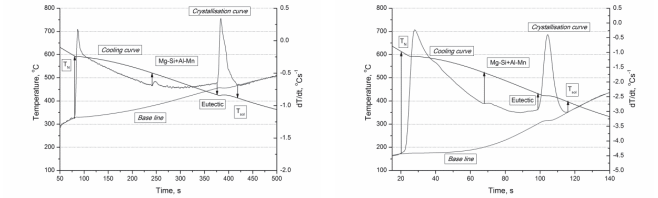

Fig. 2. Representative cooling and its first derivative curves and base line determining the critical points during solidification of the MC MgAl9Zn1 alloy solidify at: a) 0.6°Cs^{-1}; b) 2.5°Cs^{-1} cooling rate

The solidification of MC MgAl6Zn1 and MC MgAl9Zn1 alloys starts with nucleation of α-Mg dendrites. After the formation of α-Mg dendrites, phases containing mainly Mg-Si and Al-Mn occurs. Last stage in the solidification process of investigated magnesium alloys is the solidification of eutectic, as divorced or partially divorced γ-$Mg_{17}Al_{12}$ interdendritic regions and grain boundary. It should be taken of the fact that apart $Mg_{17}Al_{12}$ phase is forming from the eutectic reaction also arise $Mg_{17}Al_{12}$ phase according to the discontinuous mechanism. In both discontinuous γ phase and α+γ crystallise as multicomponent eutectic, where its content is a 32.3% of Al. At this moment when the discontinuous γ phase is formed from the surroundings, magnesium is taken, with a consequent increase in the aluminium content thus allowing the crystallisation of the basic eutectic α+γ and so on until complete crystallisation (i.e. the reaction autocatalytic).

Base on the results of combined LM, SEM and EDS analyses, which were shown in Figs 3-8, it was verified that in the structure of analysed magnesium alloys, the bright plate-shaped particle containg Al-Mn, dark polygonal-shaped particle was a Mg-Si and the irregular shaped particle extends along primary magnesium dendrites; moreover it has been noticed that grain boundaries at the final solidification regions was a $Mg_{17}Al_{12}$. Distribution of intermetallic compounds in the microstructure, such as Mg-Si and Al-Mn located on the edge of γ phase and at grain boundaries or in the interdendritic regions, indicates that these phases precipitated before eutectic reaction and simultaneous precipitation at higher temperature.

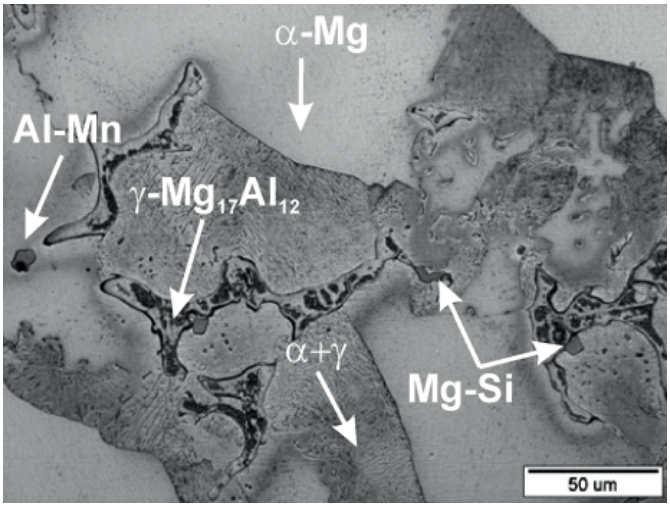

Fig. 3. Representative light microscope microstructure of MC MgAl9Zn1 alloy solidify at 0.6°Cs^{-1}

Such a sequence of crystallisation was based on similar results reported by other researchers [14-16], and equliribium phase systems [17]. Moreover, the adopted crystallisation sequence was based on results from analysis of the TDA through which is possible to estimate the amount of occurrence of structural components in the material based on the generated peaks that correspond to the amount of emitted of latent heat. If the registered peak on crystallisation curve is small, it indicates a small amount of latent heat generated and clearly indicates the presence of a small amount of the component in the structure.

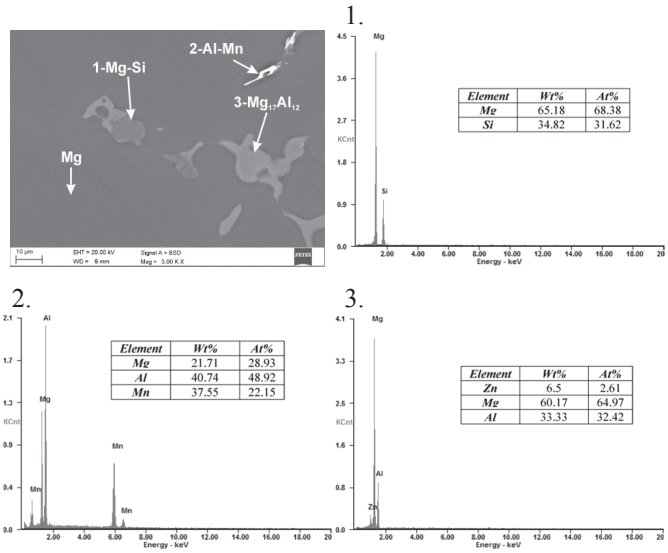

Fig. 4. Representative SEM micrographs of an MC MgAl6Zn1 alloy solidify at 0.6°Cs^{-1} cooling rate with EDS quantitative analysis results at marked points

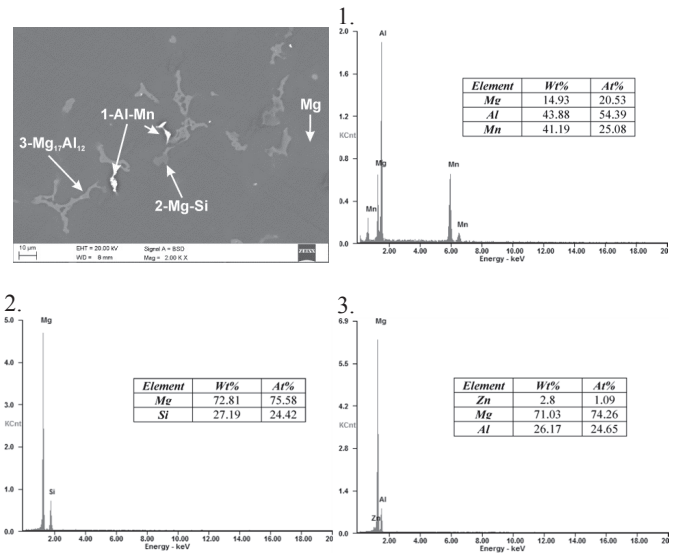

Fig. 5. Representative SEM micrographs of an MC MgAl6Zn1 alloy solidify at 2.5°Cs^{-1} cooling rate with EDS quantitative analysis results at marked points

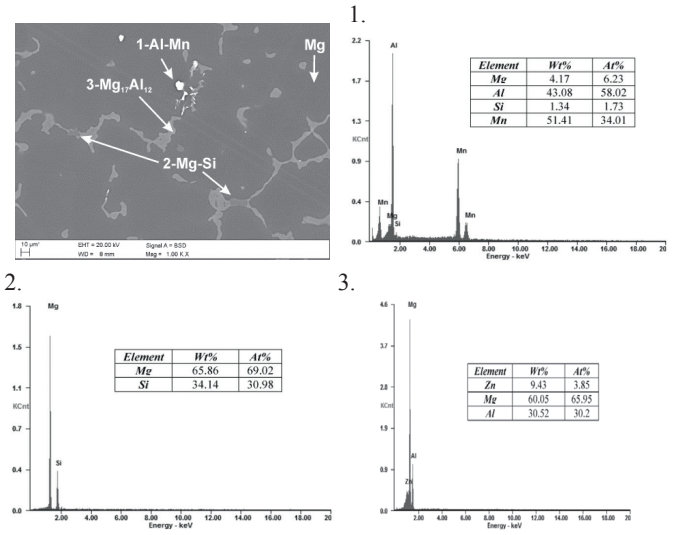

Fig. 6. Representative SEM micrographs of MC MgAl9Zn1 alloy solidify at 0.6°Cs^{-1} cooling rate with EDS quantitative analysis results at marked points

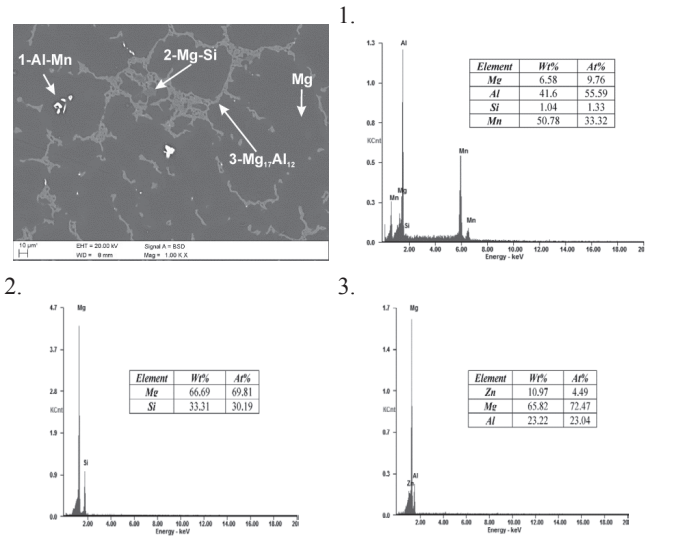

Fig. 7. Representative SEM micrographs of MC MgAl9Zn1 alloy solidify at 2.5°Cs^{-1} cooling rate with EDS quantitative analysis results at marked points

Metallographic observations of the magnesium test sample solidified at 0.6°Cs^{-1} revealed the dendritic microstructure of the α(Mg) matrix with visible eutectic regions spread within the interdenditic spaces (Fig. 8). This investigation was in agreement with the thermal analysis experiments where distinct metallurgical reactions were noted on the cooling curve, i.e., nucleation of the α(Mg) dendrites, nucleation of the phases containing Mg-Si and Al-Mn and the α(Mg)-γ($Mg_{17}Al_{12}$) eutectic. The results are in agreement with those reported by other researchers [15, 16, 18]. Image analysis showed that the average grain size of MC MgAl6Zn1 solidify at 0.6°Cs^{-1} was 160µm (Figure 8). Standard deviation represented approximately 20% of the overall grain size value that was typical for a slowly solidified test sample with a heterogeneous microstructure. Metallographic observations of the MC MgAl6Zn1 test samples that solidified at a 2.5°Cs^{-1} cooling rate revealed significant microstructural refinement caused by the thermal modification mechanism (Figures 8a, b). The grain size was reduced to 112µm as compared with 160µm for the test sample that solidified at a 0.6°Cs^{-1} cooling rate. Past studies have shown that an increase in the Al content in AZ91 alloy does not result in any grain refinement [16]. Moreover, increase the cooling rate decreases grain size of MC MgAl9Zn1 from 153µm to 103µm (Figures 8c, d). The grain size strongly depends on the increased solidification rate that reduced the time necessary for coarsening of the Mg dendrites. However, the presented results are authentic in the presented range of cooling rate.

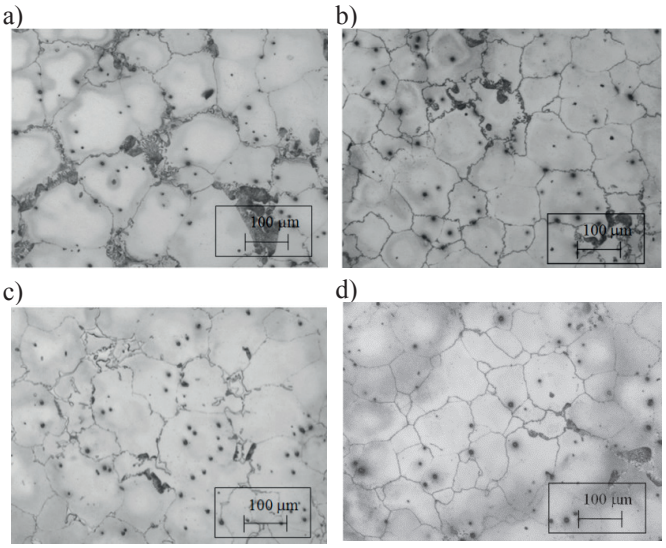

Fig. 8. Light microscope micrographs of the MC MgAl6Zn1: a-b) and MC MgAl9Zn1: c-d) alloys under 100x magnification that solidified at the following solidification rates: a, c) 0.6°Cs^{-1}; b, d) 2.5°Cs^{-1}

Figure 9 shows the X-ray diffraction analysis of MC MgAl6Zn1 and MC MgAl9Zn1 magnesium alloys. The XRD pattern presents the high intensity of magnesium reflections and low intensity of $Mg_{17}Al_{12}$. Moreover, the X-ray analysis has not indicated an occurrence of an intermetallic compound containing Mg-Si and compound containing Al-Mn. However, the comprehensive study using LM, SEM, EDS, thermal derivative analysis, literature overview and analysis of equilibrium phase system [14-20] indicate the presence of Mg-Si and Al-Mn phases in microstructure in analysed cast magnesium alloys.

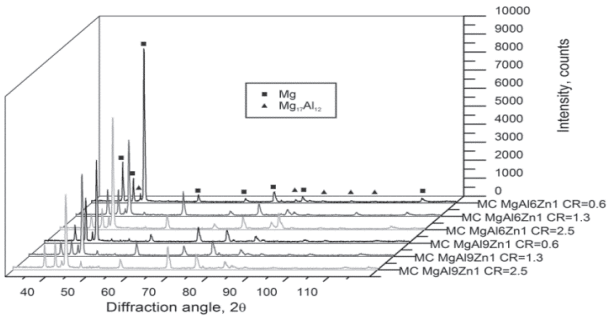

Fig. 9. X-ray diffraction pattern of analysed magnesium alloys obtained at various cooling rates (CR)

For MC MgAl6Zn1 magnesium alloy, using the natural cooling rate, the nucleation temperature of primary magnesium dendrite was recorded at around 610°C (Fig. 1). This phase grew on further cooling followed by Al-Mn and Mg-Si intermetallic precipitation approximately as 529.2°C. Further cooling caused another rapid and clear positive peak revealed on the crystallisation curve at 431.4°C due to the development of eutectic. Process finished at solidus temperature at around 423°C, where remaining liquid totally changed to the eutectic phase. It can be noticed that the increase in cooling rate increases the nucleation temperature and decreases the solidus temperature of investigated magnesium alloys (Fig. 10). The intermetallic precipitation temperature slightly increases from 529°C to 532°C with increasing cooling rate. The increase in the cooling rate increased the solidification range from about 187°C to 208°C.

Accordingly for MC MgAl9Zn1 magnesium alloy, using natural cooling rate, the nucleation temperature of primary magnesium dendrite was registered at around 592°C (Fig. 2). This phase grew on further cooling followed by Al-Mn and Mg-Si intermetallic precipitation approximately as 520.7°C. Further cooling caused next rapid, and clear positive peak revealed on the crystallisation curve at 428.2°C due to the evolution of latent heat during eutectic transformation. Process finished at solidus temperature at around 414°C. It can be noted for MC MgAl9Zn1 alloy that the increase in cooling rate increases the nucleation temperature and decreases the solidus temperature (Fig. 10). Changing the cooling rate does not significantly effect on intermetallic precipitation temperature. The solidification range increases from about 178°C to 205°C with increasing cooling rate. Moreover, increase the cooling rate increases undercooling of liquid that is a driving force behind the nucleation process. The higher the undercooling, the more nucleation is formed, which after reaching a critical value increase as the α crystal phase, which in turn generate increased amounts of latent heat. For analysed series of magnesium alloys, the thermal derivative analysis shows that the cooling rate increase does not significantly affect the eutectic transformation temperature.

Results from the thermal-derivative analysis (Table 2) present that the increases in aluminium content decrease the nucleation temperature, eutectic temperature, precipitation of Mg-Si and Al-M intermetallic phases and the solidus temperature of investigated magnesium alloys. Figure 10 represents the variation in nucleation and solidus temperatures as a function of the cooling rate of investigated magnesium alloys.

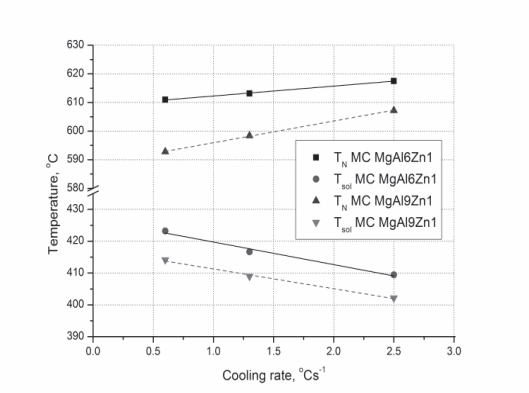

Fig. 10. Effect of cooling rate on nucleation (T_N) and solidus temperatures (T_{sol}) of investigated magnesium alloys

The coherency point for magnesium alloys was studied using CA-CCA. During the solidification step, dendrite began to evolve at the point where they impinge each on other, and a continuous network becomes coherent. At this dendrite coherency point (DCP), the analysed material behaves less like a liquid and starts to resemble a solid behaviour. According to the thermal-derivative analysis, coherency point appeared at the first minimum of the second derivative during the primary magnesium formation. Figures 11 and 12 illustrates characteristic points on the second derivative of investigated magnesium alloys due to the improved thermal contact through the stable network and a considerable difference in thermal conductivity between the liquid and solid in magnesium alloys. The dendrite coherency point determined as both a particular fraction solid (FS) and a certain temperature T_{DCP} represents an impingement of dendrites, where a strength of

TABLE 2

Thermal characterisation of investigated magnesium alloys

Investigated alloy	Cooling rate, (°Cs^{-1})	The reaction temperature			
		Liquidus, (°C)	Mg-Si+Al-Mn, (°C)	Eutectic, (°C)	Solidus, (°C)
MC MgAl6Zn1	0.6	610.9	529.2	431.4	423.1
	1.3	613.1	526.8	431.2	416.6
	2.5	617.5	532.6	428.9	409.4
MC MgAl9Zn1	0.6	592.7	520.7	428.2	414.1
	1.3	598.4	524.6	429.8	408.9
	2.5	607.2	521.8	431.1	402.1

TABLE 3

Influence of cooling rate and Al content on temperature at the dendrite coherency point and fraction solid of investigated magnesium alloys

Cooling rate, °Cs^{-1}	0.6		1.3		2.5	
	DCP, °C	FS, %	DCP, °C	FS, %	DCP, C	FS, %
MC MgAl6Zn1	609.3	3.41	607.8	6.47	610.4	14.82
MC MgAl9Zn1	590.8	5.16	594.4	7.46	591.1	13.12

mush starts to develop. The development of microstructure and casting defects in die castings and mould castings is suggested to be strongly dependent on alloy composition and crystallisation conditions. Hence, the information of DCP is crucial to understand microstructure formation during semi-solid forming and traditional casting processes.

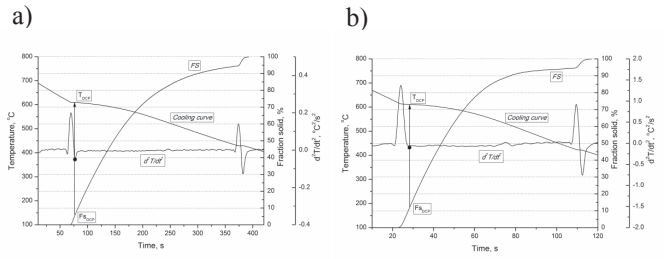

Fig. 11. Representative cooling and second derivative curves, and associated fraction solid curve of the MC MgAl6Zn1 alloy solidify at: a) 0.6°Cs^{-1}, b) 2.5°Cs^{-1} cooling rate

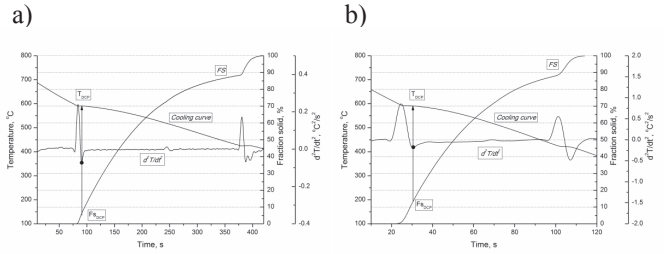

Fig. 12. Representative cooling and second derivative curves, and associated fraction solid curve of the MC MgAl9Zn1 alloy solidify at a) 0.6°Cs^{-1}, b) 2.5°Cs^{-1} cooling rate

For the one-thermocouple method, a single thermocouple located in the centre of the solidifying melt was used to determine the DCP. The increase in thermal conductivity of the solidifying melt at the DCP causes an increase in the solidification rate. The minimum value of the second derivative of temperature with respect to time (d^2T/dt^2) corresponds to the instance that a significant change occurs in the thermal conductivity of the melt. The corresponding temperature on the cooling curve is the dendrite coherency temperature (T_{DCP}).

To find a solid fraction at coherency point, the Newtonian base line has been estimated by sixth polynomial fitting $(dT/dt)BL=a_0+a_1T+a_2T^2+a_3T^3+a_4T^4+a_5T^5+a_6T^6$ between the beginning and the end of solidification in the crystallisation curve. The sixth order polynomial yields a correlation coefficient equals to 0.99. The solid fraction at DCP can be estimated from the accumulative field between the first derivative and the base line at t_{DCP}, as a portion of the area between these curves. The variations of the solid fraction matching to the dendrite coherency (f_{DCP}) as a function of the cooling rate of the analysed magnesium alloys are presented in Table 3 and plotted in Fig. 13. It can be observed that the temperature of fraction solid at coherency point decreased with increasing Al content; moreover fraction solid increased with increasing cooling rate. It can be observed for both analysed series of magnesium alloys, that the increasing cooling rate has no influence on changes in temperature at the dendrite coherency point.

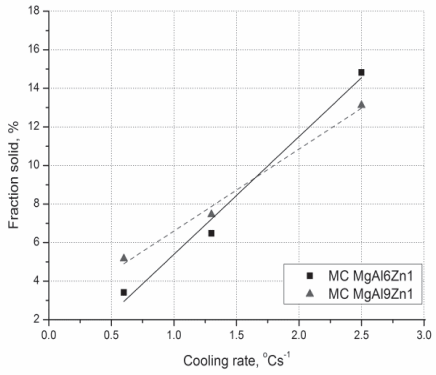

Fig. 13. Effect of cooling rate on fraction solid at the dendrite coherency point of investigated magnesium alloys

4. Conclusions

It was found that the nucleation temperature of primary magnesium dendrite increases with increasing cooling rate and decreases with increasing Al content, while solidus temperature decreases with increasing cooling rate and aluminium content. The solidification range of analysed magnesium alloys increases with increasing cooling rate.

Thanks to the knowledge of the microstructure of the thermal analysis sample, it is possible to have an idea of the microstructure, that can be expected in the real part according to its thermal behave and to the mould type. It was found that the second derivative curve could determine the dendrite coherency point. The one thermocouple method simplifies the platform and lowers the costs of thermal analysis. It is, therefore, concluded that the one thermocouple method, based on the analysis of the cooling curve, can replace the other thermal techniques such as DTA, DSC and mechanical, i.e., rheological methods for determination of the dendrite coherency point. The increase in cooling rate increases the solid fraction at dendrite coherency point; moreover increasing the aluminium content has not affected the temperature at DCP.

REFERENCES

[1] W. Martienssen, H. Warlimont, Springer Handbook of Condensed Matter and Materials Data, Berlin Heidelberg 2005.
[2] T. Rzychoń, B. Dybowski, A. Kiełbus, Arch. Metall. Mater. **60**, (1), 167-170 (2015).
[3] L.A. Dobrzański, T. Tański, Influence of Aluminium Content on Behaviour of Magnesium Cast Alloys in Bentonite Sand Mould, in: Z. Gosiewski, Z. Kulesza (Ed.), Mechatronic Systems and Materials III 2009, Solid State Phenomena (2009).
[4] Y. Ali, D. Qiu, B. Jiang, F. Pan, M.-X. Zhang, J. Alloy. Compd. **619**, 639-651 (2015).
[5] L.A. Dobrzański, B. Tomiczek, M. Pawlyta, M. Król, Arch. Metall. Mater. **59**, (1), 335-338 (2014).
[6] C. Rapiejko, B. Pisarek, T. Pacyniak, Arch. Metall. Mater. **59**, (2), 761-765 (2014).
[7] B. Dybowski, A. Kiełbus, R. Jarosz, Arch. Metall. Mater. **59**, (4), 1527-1532 (2014).
[8] M. Krupiński, B. Krupińska, K. Labisz, Z. Rdzawski, W. Borek, J. Therm. Anal. Calorim. **118**, (2),1361-1367 (2014).
[9] L.A. Dobrzański, R. Maniara, J. Sokolowski, W. Kasprzak, M. Krupiński, Z. Brytan, J. Mater. Process. Tech. **192**, 582-587 (2007).
[10] M. Szymanek, B. Augustyn, D. Kapinos, S. Boczkal, J. Nowak, Arch. Metall. Mater. **59**, (1), 317-321 (2014).
[11] United States Patent No. US 2005/0151306 A1: Method and apparatus for universal metallurgical simulation and analysis, J. H. Sokolowski, W. T. Kierkus, M. Kasprzak, W. J. Kasprzak, Jul. 14, 2005.
[12] T. Tański, K. Labisz, B. Krupińska, M. Krupiński, M. Król, R. Maniara, W. Borek, J. Therm. Anal. Calorim. (2015), DOI 10.1007/s10973-015-4871-y (in press).
[13] L. A. Dobrzański, M. Król, T. Tański, R. Maniara, Archives of Materials Science and Engineering **34**, (2), 113-116 (2008).
[14] H. Jafari, M. H. Idris, A. Ourdjini, S. Farahany, Mater. Design 50, 181-190 (2013).
[15] W. Kasprzak, J.H. Sokolowski, M. Sahoo, L.A. Dobrzański, Journal of Achievements in Materials and Manufacturing Engineering **28**, (2), 131-138 (2008).
[16] Y.C. Lee, A.K. Dahle, D.H. StJohn, Metall. Mater. Trans. A **31**, (11), 2895-2906 (2000).
[17] http://www.factsage.com
[18] M.A. Malik, K. Majchrzak, K.N. Braszczyńska-Malik, Archives of Foundry Engineering **12**, (4), 109-112 (2012).
[19] D.H. Hou, S.M. Liang, R.S., Chen, E.H. Han, C. Dong, Mater. Sci. Forum **686**, 371-377 (2011).
[20] P. Skupień, R. Rozmus, Prace Instytutu Metalurgii Żelaza **4**, 18-22 (2013).

Received: 10 November 2014.